RSC Advances

PAPER

View Article Online
View Journal | View Issue



Cite this: *RSC Adv.*, 2022, **12**, 11632

# Mechanical properties of an interpenetrating network poly(vinyl alcohol)/alginate hydrogel with hierarchical fibrous structures

An Yumin,[ab] Dong Liguo,[ab] Yang Yi[ab] and Jia Yongna*[c]

Bioinspired hierarchical fibrous structures were constructed in an interpenetrating poly(vinyl alcohol, PVA)/alginate hydrogel network to improve its mechanical properties. The interpenetrating hydrogel network with hierarchical fibrous structures was prepared by combining the confined drying method and freeze–thaw method. First, $Ca^{2+}$ cross-linked alginate formed a nano–micro hierarchical fibrous structure *via* the confined drying method. Then, PVA that was uniformly distributed among the $Ca^{2+}$–alginate chains was cross-linked by hydrogen bonding *via* the freeze–thaw method, further dividing the hierarchical fibers into finer fibers. The results of a tensile test demonstrated that both the tensile stress and fracture energy improved by more than double after the introduction of 2 wt% PVA, achieving a combination of high strength (~12.9 MPa), high toughness (~13.2 MJ $m^{-3}$) and large strain (~161.4%). Cyclic tensile tests showed that a hysteresis loop existed on the loading–unloading curves of the hydrogel along the fibrous directions, and a good self-recovery property emerged after resting for a period of time. The hydrogel with hierarchical fibrous structures constructed by alginate and PVA can be employed in biomedical applications in the future.

Received 4th October 2021
Accepted 28th March 2022

DOI: 10.1039/d1ra07368k

rsc.li/rsc-advances



## 1. Introduction

Alginate hydrogels have drawn considerable attention in tissue engineering,[1] drug delivery,[2] cell culture,[3] and soft robot[4] for their special biophysical and chemical properties similar to those of the native extracellular matrix. However, weak and brittle mechanical properties of the hydrogels limit their usage in a strength-requiring application. Numerous efforts have been devoted to improving the strength and toughness of alginate hydrogels using various energy dissipation strategies, such as interpenetrating network hydrogels[5,6] and nano-composite hydrogels.[7,8] Interpenetrating network alginate-based hydrogels consist of an ionically cross-linked rigid alginate network and a poorly cross-linked ductile network.[9–11] The strength and modulus are guaranteed by the first rigid ionically cross-linked alginate network, and the toughness and flexibility are ensured by the second ductile network. When the hydrogel is subjected to stress, energy is dissipated by fracture of the rigid ionically cross-linked alginate network at the crack tip and efficient energy transmission of the flexible network, thus preventing the expansion of the crack tip. Moreover, the mechanical behavior and energy dissipation mechanism of hydrogels can be adjusted by selecting the types of chemical bonds in the networks, such as covalent bonds, hydrogen bonds and other noncovalent bonds.[12,13] In addition, a dual physical interpenetrating network cross-linked polyvinyl alcohol (PVA)/alginate hydrogel possesses high mechanical properties while achieving drug delivery and other functional properties.[14–16] Compared with either alginate or PVA hydrogel, the dual interpenetrating network of the PVA/alginate hydrogel improved the mechanical properties considerably.

Apart from these strategies, skeletal muscle or cartilage tissues possess high strength and toughness through designing hierarchical fibrous structures from nanoscale to macroscale using simple water, collagen, proteoglycan, or protein.[17,18] Inspired by these soft tissues with highly ordered structures, researchers have increasingly investigated anisotropic hydrogels with highly ordered structures to achieve unique mechanical properties.[19] Numerous methods have been developed to construct highly ordered structures, such as employing shear force to alginate hydrogels to construct aligned rod-like tobacco mosaic virus[20] or casein networks,[21] utilizing tensile force to fabricate an ordered alginate fibrous network[22] in the materials, and magnetically controlling alginate-stabilized magnetic nanoparticles to achieve aligned pores in hydrogels.[23] In general, the mechanical properties of an anisotropic hydrogel can be tuned by the structural parameters of the anisotropic architecture, for example, oriented nanofillers, polymer chain networks or void channels.[24–26] It is expected that the mechanical properties of alginate hydrogels can be improved by

[a]*State Key Laboratory of Reliability and Intelligence of Electrical Equipment, Hebei University of Technology, Tianjin, PR China*

[b]*School of Mechanical Engineering, Hebei University of Technology, Tianjin, 300401, PR China*

[c]*School of Artificial Intelligence, Hebei University of Technology, Tianjin, 300401*

rationally selecting an interpenetrating network when constructing oriented architectures.

Here, a method combining the confined drying method and freeze–thaw method is proposed to construct hierarchically arranged fibrous structures in the interpenetrating network PVA/alginate hydrogel. The microstructures of the interpenetrating network PVA/alginate hydrogel were analyzed in detail. The anisotropic tensile mechanical properties of the interpenetrating network PVA/alginate hydrogel were studied. Cyclic tensile properties of the interpenetrating network PVA/alginate hydrogel along the fibrous structures were also studied. Besides, the self-recovery properties of the interpenetrating network PVA/alginate hydrogel with hierarchically arranged fibrous structures were also analyzed and discussed.

## 2. Experimental

### 2.1 Fabrication of the PVA/alginate hydrogel

The typical hydrogel was fabricated as follows: the PVA/alginate solution was prepared by dissolving 2 wt% sodium alginate (AR, molar mass: 198.11 g $mol^{-1}$, Aladdin, China) and 2 wt% PVA (alcoholysis degree: 72.5–74.5 mol%, molar mass: 44.05 g $mol^{-1}$, Aladdin, China) in deionized water and stirring overnight. Then, the PVA/alginate solution was poured into one reaction cell, which was fabricated by two Teflon plates (15 cm × 3 cm) with a 4 mm spacer. Then, 0.5 M calcium chloride solution (99.9%, Aladdin, China) was introduced to crosslink the alginate in the solution at the upper empty part of the reaction cell for 10 h. After that, the gel was taken out and placed into a 1.0 M calcium chloride solution for one day. Finally, both ends of the gel with a thickness of ~3.5 mm and a width of 15 cm were clamped. The distance between the two clamps was 12 cm. The gel was left in a drying box with a temperature of 25 °C and humidity of 40–60% to dry. After complete drying, the clamped portion of the gel was cut from both ends, and the dried hydrogel was allowed to swell by soaking in deionized water again. Thereafter, the freeze–thaw method was utilized to crosslink PVA. The typical process first involves the hydrogel being placed at −18 °C for 10 h, and then thawed at 25 °C for 2 h. The cooling rate was approximately 0.3 °C $min^{-1}$ from room temperature to −18 °C. The process was repeated four times and the novel hydrogel was achieved.

### 2.2 Characterization

FTIR spectra of the PVA/alginate hydrogel were recorded on a Fourier transform infrared spectrometer (FTIR; Vertex 80v, Germany) in the range of 400–4000 $cm^{-1}$ using KBr pellets. The microstructures of the PVA/alginate hydrogel with hierarchical fibrous structures were characterized by scanning electron microscopy (SEM; JSM-6510A, Japan). The tensile mechanical properties of the hydrogel were recorded with a mechanical testing system (MTS; CMT6104, China). The size of the test strips was within a length of 1–2 cm and a width of 3–4 mm. The thickness of the strips varied between 1.5 and 2 mm and the number of test samples was not less than 5. The force sensor was 100 N and loading rate was 20 mm $min^{-1}$. The cyclic tensile tests were presented at a maximum strain of 30% at the same loading and unloading rate of 20 mm $min^{-1}$, and the tensile cycle was conducted 50 times. A single loading–unloading test was carried out to assess the self-recovery properties of the PVA/alginate hydrogel. The samples were initially stretched to a predetermined strain (30%) at a stretching rate of 20 mm $min^{-1}$ and then unloaded at the same rate. After that, the test samples were relaxed at room temperature for a certain waiting period (0, 10, 20 or 30 min) before the next loading process.

## 3. Results and discussion

To improve the mechanical properties of the alginate hydrogel, hierarchically fibrous structures were constructed in the interpenetrating network PVA/alginate hydrogel through a two-step method. First, the alginate chains distributed randomly among PVA/alginate solutions were cross-linked by $Ca^{2+}$ in the reaction cell (Fig. 1a). After this, the $Ca^{2+}$-crosslinked alginate chains were still distributed in a disorderly manner in the hydrogels. In order to orient the $Ca^{2+}$-crosslinked alginate chains, a confined drying method was utilized. With the evaporation of water, the length of the hydrogel could not be changed due to the fixation, but the width was gradually narrowed. In the confined drying process, a tensile force is generated gradually, which drives the $Ca^{2+}$-crosslinked alginate chains to align and self-assemble into a hierarchical fibrous structure, as schematically depicted in Fig. 1b. Simultaneously, PVA is distributed uniformly among the hierarchical fibrous structures due to hydrogen bonding between PVA and alginate. Finally, a repeated freeze–thaw process was

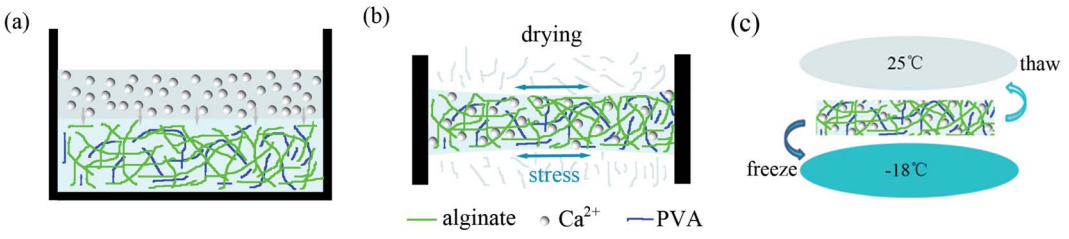


Fig. 1 Schematic diagrams of the preparation process for the interpenetrating network hydrogel with hierarchical fibrous structures: randomly distributed alginate chains in the PVA/alginate solution were crosslinked by $Ca^{2+}$ (a), alginate hierarchical fibrous structures were formed by the confined drying method (b), and the interpenetrating network hydrogel with hierarchical fibrous structures was formed after the freeze–thaw method (c).

utilized to cross-link PVA chains within the hierarchical fibrous structures, as depicted in Fig. 1c. By combining the confined drying method and freeze–thaw method, hierarchically fibrous structures with an interpenetrating network were achieved in the PVA/alginate hydrogel.

Fig. 2 shows the typical FTIR spectra of alginate, PVA and the interpenetrating network PVA/alginate hydrogel. As shown in the spectra of alginate, the strong absorption peaks around 3431, 2920, 1620, 1413 and 1029 $cm^{-1}$ are related to the stretching vibration of –OH, –C–H, –COO– (asymmetric), –COO– (symmetric), and C–O–C, respectively. Compared to alginate, there was an obvious shift of –COO– stretching bands to higher wavenumbers for the interpenetrating network PVA/alginate hydrogel, indicating the formation of ionic bonding between $Ca^{2+}$ and $–COO^-$ of alginate.[16] The PVA mainly showed bands at 3396 $cm^{-1}$ (–OH stretching), 2918 $cm^{-1}$ (–CH stretching) and 1045 $cm^{-1}$ (–C–O– stretching). The peak corresponding to –OH groups shifted to a higher wavenumber in the interpenetrating network PVA/alginate hydrogel due to the hydrogen bonding interactions between PVA and alginate molecular chains, as discussed in a previous report.[27] The formation of these ionic bonds and hydrogen bonds in the PVA/alginate hydrogel was expected to improve the mechanical properties.

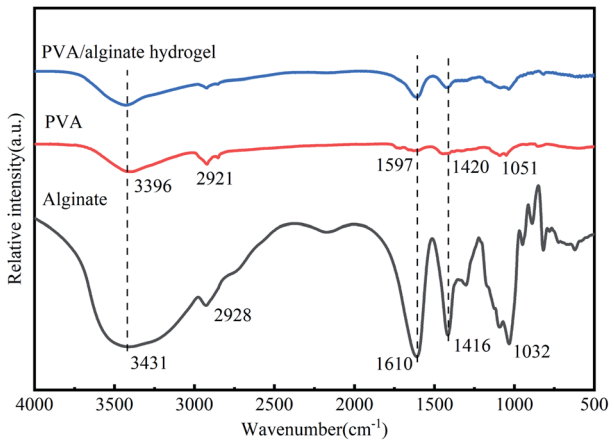


Fig. 2 Typical FTIR spectra of alginate, PVA and the interpenetrating network PVA/alginate hydrogel with hierarchical fibrous structures.

Fig. 3 shows typical SEM images of the PVA/alginate hydrogel at micro scale. It was easy to see that the $Ca^{2+}$-crosslinked alginate chains formed a fibrous microfilament after the fabrication process, as depicted in Fig. 3a. A similar microstructure was found in a previously reported fibrous alginate hydrogel.[28] After adding PVA, the fibrous structures of the hydrogel began to split and there were obvious branches between two fibrous microfilaments, as depicted in Fig. 3b–d. To further show the hierarchical fibrous structures in the interpenetrating network hydrogel clearly, high magnification images are shown in Fig. 4b–d. It was clearly found that each branch of the fibrous microfilament contained several submicron-sized thin fibers. The diameters of the fibrous microfilament of the hydrogel with 1 wt%, 2 wt%, 4 wt% of PVA were about 3.0 μm, 2.4 μm, and 2.9 μm, respectively. With the increase in PVA, the diameters of the branch of fibrous microfilament were about 1.4 μm, 0.7 μm, and 1.9 μm, respectively. Simultaneously, the diameters of the submicron-sized fibers were about 0.6 μm, 0.2 μm, and 0.2 μm, as depicted in Fig. 4b–d, respectively. Compared with alginate

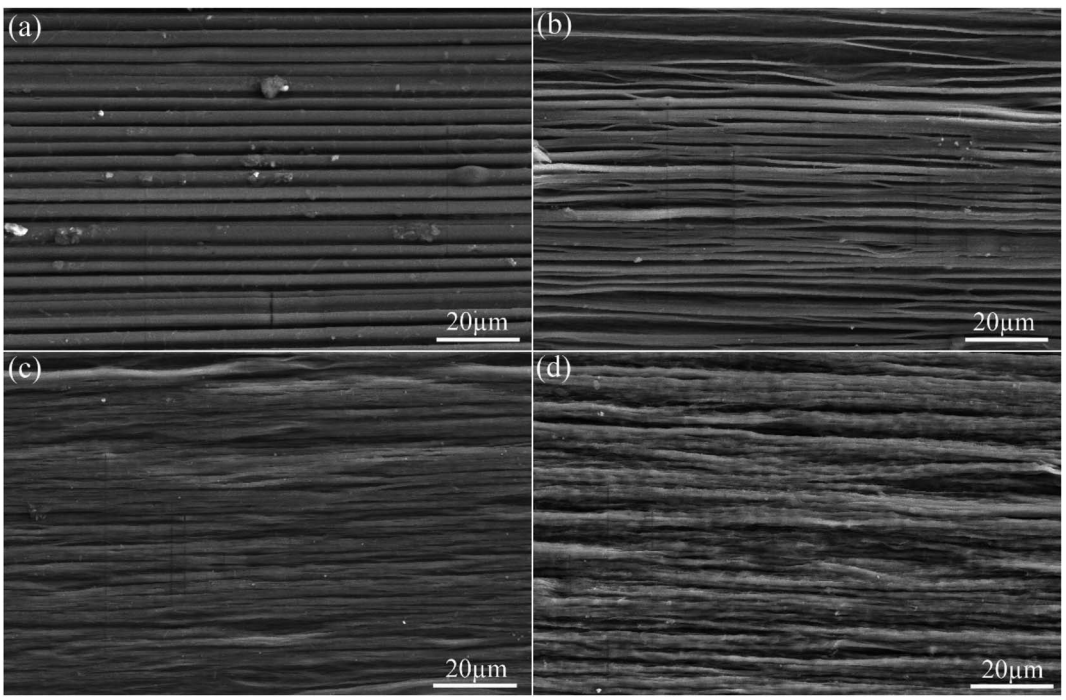


Fig. 3 Typical SEM images of the interpenetrating network PVA/alginate hydrogel with hierarchical fibrous structures containing 0 wt% (a) 1 wt% (b), 2 wt% (c), 4 wt% (d) of PVA.

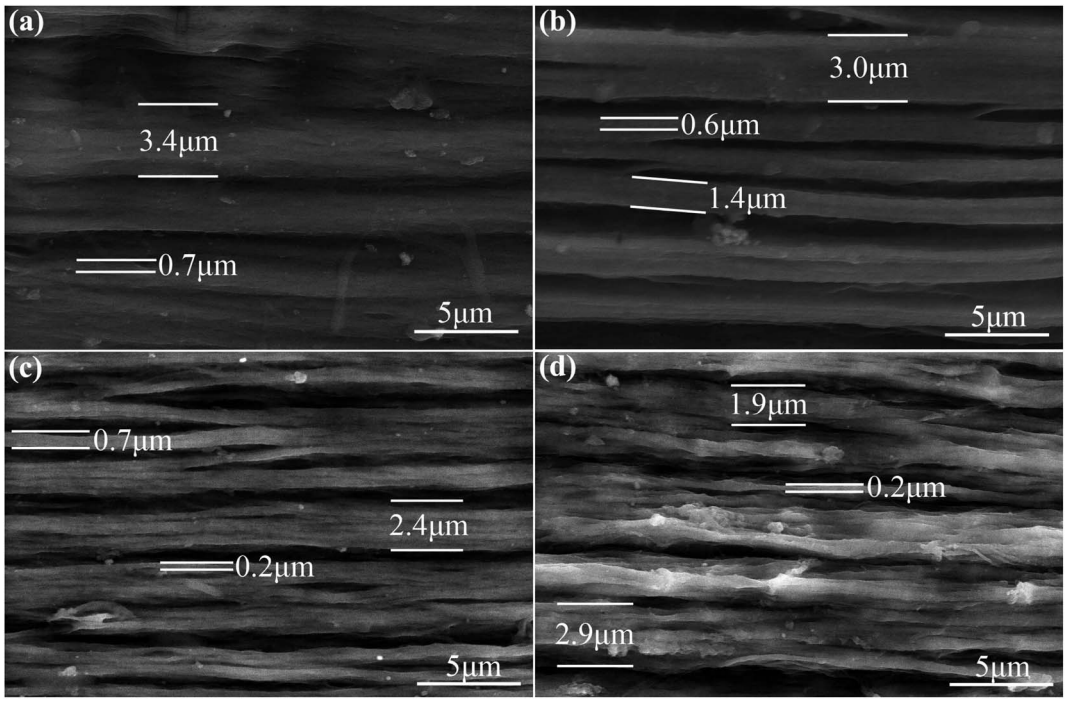


Fig. 4 Typical high magnification SEM images of the interpenetrating network PVA/alginate hydrogel with hierarchical fibrous structure containing 0 wt% (a) 1 wt% (b), 2 wt% (c), 4 wt% (d) of PVA.

hydrogel with hierarchical fibrous structures (Fig. 4a), the diameters of fibrous structures became finer after the introduction of PVA. The reason might be the PVA chains uniformly distributed inside the alginate chains were cross-linked during the repeated freezing and thawing process, which resulted in the bifurcation of the alginate chains that had been distributed in the fibrous form.

Typical stress–strain profiles of the interpenetrating network PVA/alginate hydrogel with a hierarchical fibrous structure are shown in Fig. 5a. The tensile mechanical properties of the interpenetrating network PVA/alginate hydrogel along and vertical to the fibrous directions were studied to evaluate the anisotropy in mechanical response caused by hierarchical fibrous structures. It was clear that the stress along the fibrous structures was larger than that vertical to the fibrous structures, as depicted in Fig. 5b. Simultaneously, the tensile stress tended to increase first and then decrease when the added amount of PVA did not exceed 4 wt%. The stress increased more than double after adding 2 wt% PVA to construct hierarchical fibrous structures in the interpenetrating network PVA/alginate hydrogel, which was improved from 5.3 MPa to 12.9 MPa. The reason might be that a small amount of PVA in hierarchical fibrous structures of alginate will bifurcate and refine the fiber structures during the cross-linking process. However, when the PVA increased to a certain amount, the fiber diameter becomes coarse. As depicted in Fig. 5c, the strain of the interpenetrating network PVA/alginate hydrogel along the fibrous structures was lower than that vertical to the fibrous structures, which was contrary to the relationship between stress and microstructure. The strain of the interpenetrating network hydrogel along the fibrous structures changed a little, ranging from 122.2% to 161.4% for the hydrogel with different mass fractions of PVA. The strain of the hydrogel vertical to the fibrous structures was reduced from 209.8% to 152.4% when the mass fractions of PVA increased from 0 wt% to 4 wt%. Moreover, the area enclosed by the stress–strain profiles was employed to analyze the fracture energy of the interpenetrating network PVA/alginate hydrogel (Fig. 5d). The maximum fracture energy (13.2 MJ $m^{-3}$) also appeared along the directions of the fibrous structures of the hydrogel with 2 wt% PVA, which was more than double that of alginate without PVA. The minimum fracture energy was 2.7 MJ $m^{-3}$, occurring in the direction perpendicular to the fibrous structures of the hydrogel with 4 wt% PVA. The relationship between the fracture energy and PVA content was nearly the same as that of stress and PVA content. The detailed results are shown in Table 1.

During cyclic loading–unloading tests, one large hysteresis loop appeared in the first loading–unloading cycle (Fig. 6a, c and e), which implied energy dissipation was involved in the deformation of the interpenetrating network PVA/alginate hydrogel with hierarchical fibrous structures. The reason might be the $Ca^{2+}$–alginate ionic bonds and hydrogen bonds between alginate and PVA were disrupted, dissipating energy during the loading and unloading processes. The dissipation energy was calculated as the area enclosed by the hysteresis curves during one cyclic loading–unloading test.[29,30] In the following cycles, a substantial decrease emerged for the dissipated energy and gradually reached a stable value, as depicted in Fig. 6b, d and f. However, the maximum stress of the PVA/alginate hydrogel with 1 wt% and 2 wt% PVA first decreased and then increased gradually with cyclic loading while the stress

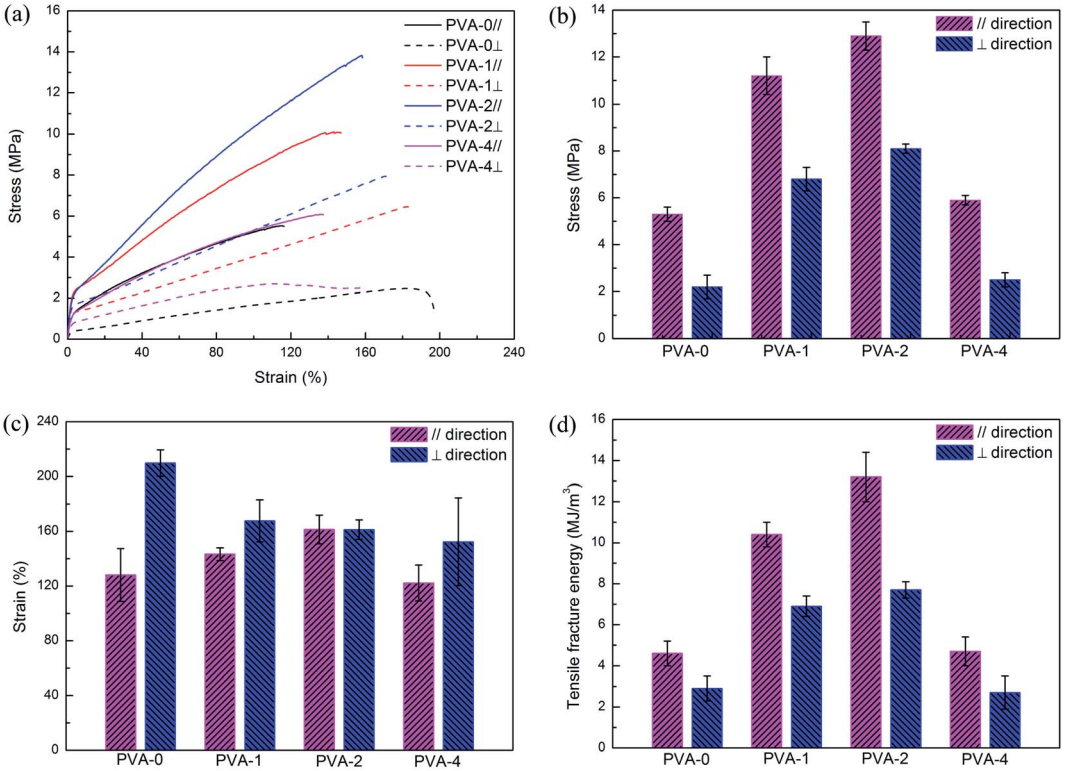


Fig. 5 Mechanical properties of the interpenetrating network PVA/alginate hydrogels with different mass fractions of PVA along (||) and perpendicular (⊥) to the fibrous directions: tensile stress–strain curves (a), tensile stress (b), tensile strain (c) and tensile fracture energy (d).

of the hydrogel with 4 wt% PVA gradually decreased to a stable value. After fifty loading–unloading cycles, the dissipated energy was not less than 0.04 MJ $m^{-3}$, and the minimum stress was more than 2.0 MPa. Simultaneously, both the dissipated energy and maximum stress of the interpenetrating network PVA/alginate hydrogel with 2 wt% PVA were larger than those of the other two types of hydrogels, which was consistent with the results obtained from the tensile stress–strain relationship.

Single loading–unloading tests with a predetermined strain of 30% were reiterated after different resting times to explore the recovery behavior of the interpenetrating network PVA/alginate hydrogel. Compared with the results of the original sample, one significant decrease emerged for both the dissipated energy and elastic modulus of the interpenetrating network PVA/alginate hydrogel between two consecutive loadings without resting, as depicted in Fig. 7. After the samples rested from 0 to 30 min, both the dissipated energy and elastic modulus of the interpenetrating network PVA/alginate hydrogel gradually recovered, even slightly surpassing that of their original samples. For example, the dissipated energy and elastic modulus of the interpenetrating network PVA/alginate hydrogel with 4 wt% PVA increased from 1.03 MJ $m^{-3}$ and 0.89 MPa to 1.33 MJ $m^{-3}$ and 0.95 MPa after resting for 30 min, respectively. The recovery of the mechanical properties of the interpenetrating network PVA/alginate hydrogel indicated that both the $Ca^{2+}$–alginate ionic bonds and hydrogen bonds between PVA and alginate were almost reversible. Moreover, the improvement of tensile dissipated energy and elastic modulus might be attributed to a unique stiffening of the interpenetrating network PVA/alginate hydrogel with hierarchical fibrous structures during the periodic deformation process.

Table 1 Tensile mechanical properties of the interpenetrating network PVA/alginate hydrogel with different mass fractions of PVA along (||) and perpendicular (⊥) to the fibrous directions

| Material | Stress (MPa) | Strain (%) | Fracture energy (MJ $m^{-3}$) |
|---|---|---|---|
| PVA-0 wt% \|\| | 5.3 ± 0.3 | 128.1 ± 19.3 | 4.6 ± 0.6 |
| PVA-0 wt% ⊥ | 2.2 ± 0.5 | 209.8 ± 9.7 | 2.9 ± 0.6 |
| PVA-1 wt% \|\| | 11.2 ± 0.8 | 143.3 ± 4.7 | 10.4 ± 0.6 |
| PVA-1 wt% ⊥ | 6.8 ± 0.5 | 167.7 ± 15.4 | 6.9 ± 0.5 |
| PVA-2 wt% \|\| | 12.9 ± 0.6 | 161.4 ± 10.5 | 13.2 ± 1.2 |
| PVA-2 wt% ⊥ | 8.1 ± 0.2 | 161.3 ± 7.1 | 7.7 ± 0.4 |
| PVA-4 wt% \|\| | 5.9 ± 0.2 | 122.2 ± 13.1 | 4.7 ± 0.7 |
| PVA-4 wt% ⊥ | 2.5 ± 0.3 | 152.4 ± 32.1 | 2.7 ± 0.8 |

For alginate hydrogel, the $Ca^{2+}$ crosslinked alginate chains were arranged directionally, and assembled into hierarchical fibrous structures under the tensile stress whether by confined drying or stretching, as depicted in Fig. 8a. After the construction of the hierarchical fibrous structures, the mechanical properties of the hydrogel were improved significantly. After the introduction of PVA, the hydroxyl groups on the surface of PVA form hydrogen bonds with the oxygen-containing groups on the surface of alginate to ensure that the PVA chains evenly dispersed among nano or micro scale fibrous structures. In the

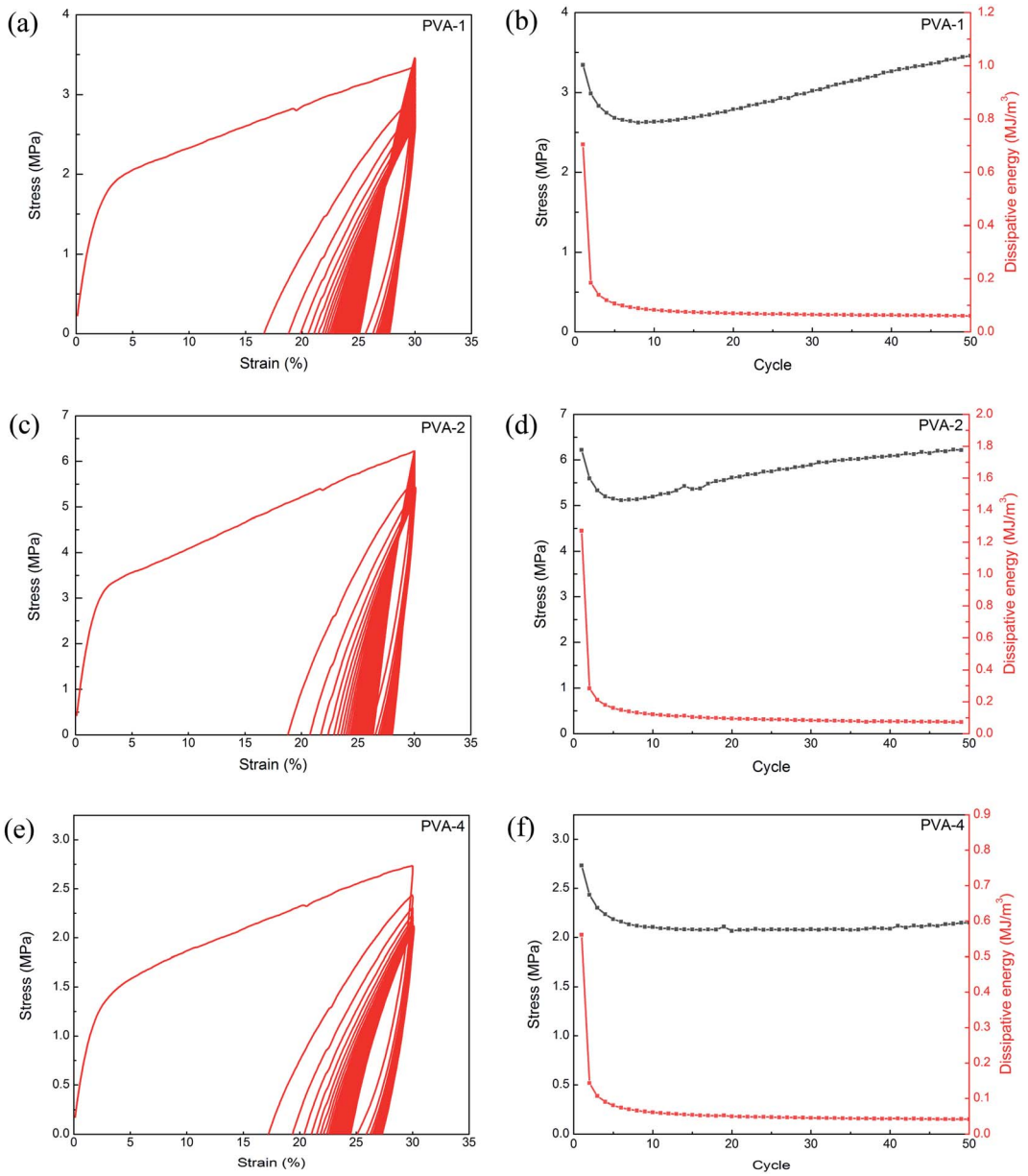


Fig. 6 Cyclic loading–unloading curves, dissipated energy and maximum stress for fifty successive loading–unloading cycles of the interpenetrating network PVA/alginate hydrogels with 1 wt% (a and b), 2 wt% (c and d), and 4 wt% (e and f) of PVA.

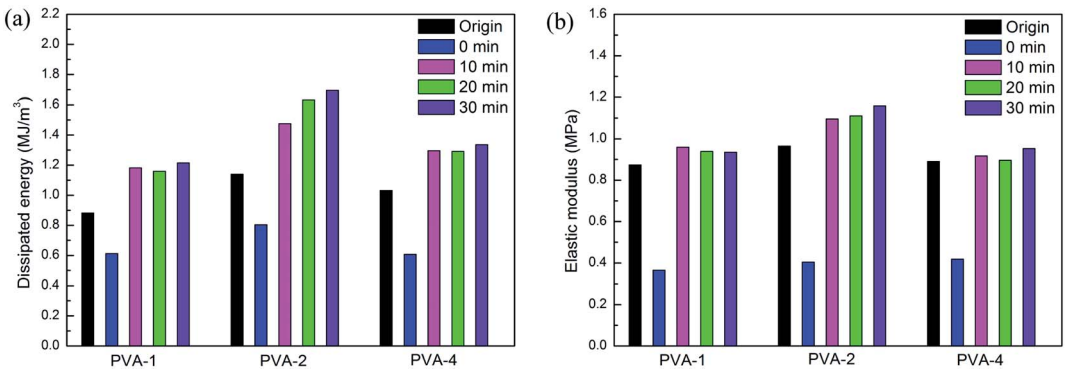


Fig. 7 Dissipated energy (a) and elastic modulus (b) of a single loading–unloading test at a strain of 30% after different resting times for the interpenetrating network PVA/alginate hydrogel with hierarchical fibrous structures.

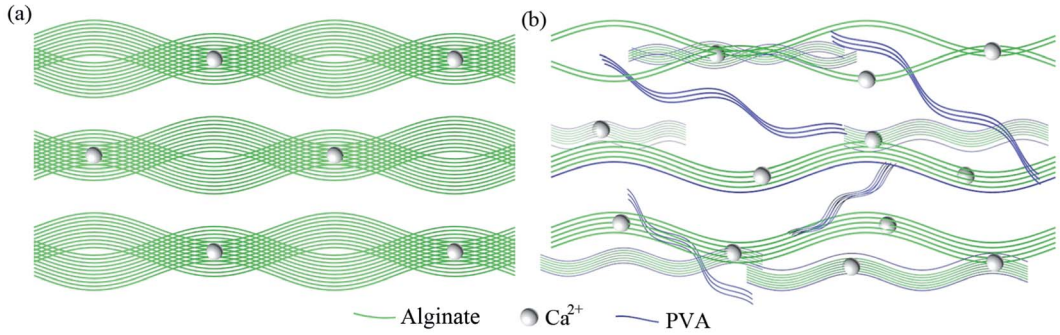


Fig. 8 Schematic diagrams of the alginate hydrogel (a) and the interpenetrating network PVA/alginate hydrogel (b) with hierarchical fibrous structures.

repeated freeze–thaw process, hydrogen bonds gradually formed between adjacent PVA chains. On the one hand, the interpenetrating network was formed in the PVA/alginate hydrogel. On the other hand, hierarchical fibrous structures of the alginate chains were split into finer fibrous structures at the nano or micro scale. These changes further improved the tensile mechanical properties of the alginate hydrogel along and perpendicular to the fibrous directions.

## 4. Conclusion

An interpenetrating network PVA/alginate hydrogel with hierarchically arranged fibrous structures was achieved by combining the confined drying method and freeze–thaw method. After the construction of hierarchically arranged $Ca^{2+}$–alginate fibrous structures in the confined drying method, hydrogen bond cross-linked PVA bifurcated and refined the fiber structures in the repeated freeze–thaw process. The tensile tests showed that the mechanical properties both along and perpendicular to the fibrous directions were improved by more than double after the construction of hierarchically arranged fibrous structures in the interpenetrating network PVA/alginate hydrogel. Simultaneously, a combination of high strength (~12.9 MPa), high toughness (~13.2 MJ $m^{-3}$) and large strain (~161.4%) was achieved. Cyclic tensile tests demonstrated that an energy dissipation mechanism existed in the loading–unloading curves of the interpenetrating network PVA/alginate hydrogel along the fibrous directions, and a good self-recovery property emerged after resting for 30 min. Our work provides a general method or strategy for improving the mechanical properties of alginate hydrogels and the hydrogels with hierarchical fibrous structures might find bioapplications in future.

## Conflicts of interest

There are no conflicts to declare.

## Acknowledgements

The authors are grateful for the support from National Natural Science Foundation of China (no. 51802072, 41804118), Natural Science Foundation of Hebei Province (no. E2020202128).

## References

1 V. A. Henrique, N. S. Binulal, D. Ivan, T. B. Conor, J. O. Fergal and J. K. Daniel, Anisotropic Shape-Memory Alginate Scaffolds Functionalized with Either Type I or Type II Collagen for Cartilage Tissue Engineering, *Tissue Eng., Part A*, 2017, **23**, 55–68.
2 K. Y. Lee and D. J. Mooney, Alginate: Properties and Biomedical Applications, *Prog. Polym. Sci.*, 2012, **37**, 106–126.
3 L. J. Macdougall, P. M. Maria, S. Joshua, I. Maria, A. H. Judith, O. Rachel, M. R. Stephen and P. D. Andrew, Self-healing, Stretchable and Robust Interpenetrating Network Hydrogels, *Biomater. Sci.*, 2018, **6**, 2932–2937.
4 W. J. Zheng, N. An, J. Yang, J. Zhou and Y. M. Chen, Tough Alginate/poly (*N*-isopropylacrylamide) Hydrogel with Tunable LCST for Soft Robotics, *ACS Appl. Mater. Interfaces*, 2015, **7**(3), 1758–1764.
5 Y. Zhuang, F. Yu, H. Chen, J. Zheng, J. Ma and J. Chen, Alginate/graphene Double-Network Nanocomposite Hydrogel Beads with Low-swelling, Enhanced Mechanical Properties, and Enhanced Adsorption Capacity, *J. Mater. Chem. A*, 2016, **4**, 10885–10892.
6 Q. Zheng, L. Zhao, J. Wang, S. Wang, Y. Liu and X. Liu, High-Strength and High-Toughness Sodium Alginate/polyacrylamide Double Physically Crosslinked Network Hydrogel with Superior Self-healing and Self-recovery Properties Prepared by a One-pot Method, *Colloids Surf., A*, 2020, **589**, 124402.
7 Q. Huang, S. Liu, K. Li, I. Hussain, F. Yao and G. Fu, Sodium Alginate/carboxyl-Functionalized Graphene Composite Hydrogel *via* Neodymium Ions Coordination, *J. Mater. Sci. Technol.*, 2017, **33**, 821–826.
8 L. Meng, C. Shao and J. Yang, Ionically Cross-linked Silk Microfibers/alginate Tough Composite Hydrogels with Hierarchical Structures, *ACS Sustainable Chem. Eng.*, 2018, **6**, 16788–16796.
9 J. Y. Sun, X. H. Zhao, W. R. K. Illeperuma, O. Chaudhuri, K. H. Oh, D. J. Mooney, J. J. Vlassak and Z. G. Suo, Highly Stretchable and Tough Hydrogels, *Nature*, 2012, **498**, 133–136.
10 C. H. Yang, M. X. Wang, H. Haider, J. H. Yang, J. Y. Sun, Y. M. Chen, J. Zhou and Z. Suo, Strengthening Alginate/

polyacrylamide Hydrogels Using Various Multivalent Cations, *ACS Appl. Mater. Interfaces*, 2013, **5**, 10418–10422.

11 S. Naficy, S. Kawakami, S. Sadegholvaad, M. Wakisaka and G. M. Spinks, Mechanical Properties of Interpenetrating Polymer Network Hydrogels Based on Hybrid Ionically and Covalently Crosslinked Networks, *J. Appl. Polym. Sci.*, 2013, **4**, 2504–2513.

12 W. Wang, Y. Zhang and W. Liu, Bioinspired Fabrication of High Strength Hydrogels from Non-covalent Interactions, *Prog. Polym. Sci.*, 2017, **71**, 1–25.

13 E. S. Dragan, Design and Applications of Interpenetrating Polymer Network Hydrogels, *Chem. Eng. J.*, 2014, **243**, 572–590.

14 X. Jiang, N. Xiang, H. Zhang, Y. Sun, Z. Lin and L. Hou, Preparation and Characterization of Poly(vinyl alcohol)/sodium Alginate Hydrogel with High Toughness and Electric Conductivity, *Carbohydr. Polym.*, 2018, **186**, 377–383.

15 X. Li, M. Shu, H. Li, X. Gao, S. Long, T. Hu and C. Wu, Strong, Tough and Mechanically Self-recoverable Poly(vinyl alcohol)/alginate Dual-physical Double-Network Hydrogels with Large Cross-link Density Contrast, *RSC Adv.*, 2018, **8**, 16674–16689.

16 S. Hua, H. Ma, X. Li, H. Yang and A. Wang, PH-sensitive Sodium Alginate/poly(vinyl alcohol) Hydrogel Beads Prepared by Combined $Ca^{2+}$ Crosslinking and Freeze-thawing Cycles for Controlled Release of Diclofenac Sodium, *Int. J. Biol. Macromol.*, 2010, **46**, 517–523.

17 Z. Zhao, R. Fang, Q. Rong and M. Liu, Bioinspired Nanocomposite Hydrogels with Highly Ordered Structures, *Adv. Mater.*, 2017, **29**, 1703045.

18 S. Jana, S. K. L. Levengood and M. Zhang, Anisotropic Materials for Skeletal-Muscle-Tissue Engineering, *Adv. Mater.*, 2016, **28**, 10588–10612.

19 K. Sano, Y. Ishida and T. Aida, Synthesis of Anisotropic Hydrogels and Their Applications, *Angew. Chem., Int. Ed.*, 2018, **57**, 2532–2543.

20 Y. Wu, Z. Jiang, X. Zan, Y. Lin and Q. Wang, Shear Flow Induced Long-range Ordering of Rod-like Viral Nanoparticles within Hydrogel, *Colloids Surf., B*, 2017, **158**, 620–626.

21 Y. Takayama and N. Kato, Shear-induced Structuring for Multiple Parallel Gel Filaments Obtained from Casein-alginate Hybrids, *Langmuir*, 2018, **34**, 13352–13360.

22 Y. He, N. Zhang, Q. Gong, H. Qiu, W. Wang, Y. Liu and J. Gao, Alginate/graphene Oxide Fibers with Enhanced Mechanical Strength Prepared by Wet Spinning, *Carbohydr. Polym.*, 2012, **88**, 1100–1108.

23 G. Margolis, B. Polyak and S. Cohen, Magnetic Induction of Multiscale Anisotropy in Macroporous Alginate Scaffolds, *Nano Lett.*, 2018, **18**, 7314–7322.

24 Y. Jiang, Y. Zhu, H. Li, Y. Zhang, Y. Shen, T. Sun, *et al.*, Preparation and Enhanced Mechanical Properties of Hybrid Hydrogels Comprising Ultralong Hydroxyapatite Nanowires and Sodium Alginate, *J. Colloid Interface Sci.*, 2017, **497**, 266–275.

25 T. Inadomi, S. Ikeda, Y. Okumura, H. Kikuchi and N. Miyamoto, Photo-induced Anomalous Deformation of Poly (*N*-isopropylacrylamide) Gel Hybridized with an Inorganic Nanosheet Liquid Crystal Aligned by Electric Field, *Macromol. Rapid Commun.*, 2014, **35**, 1741–1746.

26 K. J. De France, T. Hoare and E. D. Cranston, Review of Hydrogels and Aerogels Containing Nanocellulose, *Chem. Mater.*, 2017, **29**, 4609–4631.

27 X. Jing, H. Li, H. Mi, P. Feng, X. Tao, Y. Liu, *et al.*, Enhancing the Performance of a Stretchable and Transparent Triboelectric Nanogenerator by Optimizing the Hydrogel Ionic Electrode Property, *ACS Appl. Mater. Interfaces*, 2020, **12**(20), 23474–23483.

28 M. T. I. Mredha, Y. Z. Guo, T. Nonoyama, T. Nakajima, T. Kurokawa and J. P. Gong, A Facile Method to Fabricate Anisotropic Hydrogels with Perfectly Aligned Hierarchical Fibrous Structures, *Adv. Mater.*, 2018, **30**, 1704937.

29 Y. An, L. Gao and T. Wang, Graphene Oxide/alginate Hydrogel Fibers with Hierarchically Arranged Helical Structures for Soft Actuator Application, *ACS Appl. Nano Mater.*, 2020, **3**, 5079–5087.

30 S. Liu, A. K. Bastola and L. Li, A 3D Printable and Mechanically Robust Hydrogel Based on Alginate and Graphene Oxide, *ACS Appl. Mater. Interfaces*, 2017, **9**, 41473–41481.